Proceedings of the 21st ICSMGE, Vienna, Austria, 14 – 19 June 2026. Pistrol, Adam & Schweiger (eds.)
Published by: ÖGG, Austrian Society for Geomechanics, Salzburg, Austria, ISBN 978-3-9503898-4-5
https://doi.org/10.53243/ICSMGE2026-506

Influence of Back Pressure on Degree of Saturation of Sand Triaxial Experiments

Mohammed Elnur, **Khalid A. Alshibli**
Department of Civil and Environmental Engineering, University of Tennessee, Knoxville, USA, Alshibli@utk.edu

ABSTRACT: Back pressure (BP) is used to saturate triaxial specimens before the shearing phase. A high BP is commonly used in the laboratory to ensure a high degree of saturation. Most soil deposits in the field for Civil Engineering applications have a low pore water pressure in the range of 30 to 50 kPa. The principles of soil mechanics postulate that the value of BP does not affect the behavior of triaxial specimens as long as the effective confining pressure is kept constant. This paper investigates the influence of BP on the behavior of uniform saturated sand tested using axisymmetric triaxial compression (ATC). 3D synchrotron micro-computed tomography (SMT) technique was used to acquire 3D scans while shearing the specimens to probe localized events that are completely missed or misinterpreted when analyzing ATC measurements based on global standard measurements. Specimens tested under low BP exhibited a large pore air volume change, which was not detected by ASTM standard measurements for triaxial cells. The paper discusses the influence of BP on the deformation mode of the specimens using rich SMT images and sheds light on the change of degree of saturation for specimens tested at low BP, and compares the behavior of specimens tested at high BP.

KEYWORDS: Air growth, volume measurement system.

1 INTRODUCTION

The constitutive behavior of soils is typically studied under either at dry, partially saturated, or saturated soil mechanics frameworks, depending on the degree of saturation of the soil. The transition point between saturated and unsaturated states is a point of contention. Many of the early proposed theories consider that the drop in the degree of saturation (S) below 100% is the point at which the unsaturated soil mechanics should take effect (Bishop et al., 1960). Realistically, it's very difficult to achieve a 100% saturation degree, whether in a laboratory setup or at in-situ conditions. More recent studies recognized the oversimplification of identifying a single value for S as a transition point between the two frameworks, neglecting the soil characteristics. A more general consensus was to utilize the variation in water content with matric suction; known as the soil-water characteristics curve (SWCC); to identify the critical points in the constitutive behavior of unsaturated soils (Fredlund, 2019). Non-zero air-entry and air-exclusion values for metric suction are accepted as the limit at which the soil completely transitions to and from an unsaturated state, for drying or wetting conditions, respectively (Lloret-Cabot et al., 2018, Vanapalli et al., 1996).

In practice, it is difficult to determine the degree of saturation directly when conducting axisymmetric triaxial compression (ATC) experiments without disturbing the soil. Achieving full saturation in ATC testing is typically assessed by measuring Skempton's pore-pressure coefficients (Skempton, 1954). Many standards; including ASTM D7181; consider the specimen fully saturated when a 95% B-value is achieved. The assessment of S is typically performed during the saturation phase before shearing the specimen. During the shearing stage, S is not assessed; only volume change and pore water pressure are measured at that stage, assuming that full saturation conditions are continuously maintained until the end of testing, especially in cases of contractive volumetric behavior.

X-ray computed tomography (CT) imaging has emerged in recent decades as a powerful non-destructive method to investigate localized behavior and assess the change in degree of saturation (Kido and Higo, 2017, Takano et al., 2015). The objective of this paper is to investigate the influence of back pressure on the evolution of S during ATC testing of sand using CT imaging to assess the change in S at different stages of loading. Two different back pressures (BPs) were selected to represent laboratory and field conditions. A high back pressure is used in laboratories to achieve a higher S at a shorter period. The zone of interest for the majority of geotechnical projects typically extends a few meters below the ground surface, where pore water pressure in these regions is low; hence, a low back pressure was used to mimic field conditions.

2 MATERIALS

Three types of natural silica sand were used in this study to investigate whether the experimental results are dependent on particle morphology and particle size distribution. The first sand (S1) is F35 Ottawa sand mined from Ottawa, Illinois, USA, and marketed by US Silica company. The second sand (S2) is Columbia Grout sand, marketed by U.S. Silica Company. Both *S1* and *S2* sands were sieved to obtain a size fraction between U.S. sieves #40 (0.429 mm) and #50 (0.297 mm), representing a narrow gradation (uniform) with a mean grain size (d_{50}) of 0.360 mm and a uniformity coefficient (C_u) of ~1.2. *S1* sand represents a more rounded sand, while *S2* represents a more angular sand (Alshibli et al., 2015). *S3* sand is a Columbia grout sand; however, unlike *S2*, the size fraction for *S3* was between U.S. sieves #20 (0.850 mm) and #200 (0.075 mm), leading to a wider particle gradation (non-uniform) with a d_{50} of 0.546 mm and a C_u of 3.0. The use of *S2* and *S3* sand reduces the particle morphology effect, as both sands are from the same source but with different particle gradations.

Table 1. Summary of ATC experiments at initial conditions, including dry density (ρ_d), cell pressure (σ_3), back pressure (BP), and the initial degree of saturation.

Specimen	ρ_d (g/cm^3)	σ_3 (kPa)	*BP* (kPa)	*S* (%)
S1-30	1.680	74	30	90.1
S1-300	1.660	350	298	98.5
S2-30	1.640	80	30	92.8
S2-300	1.650	350	298	99.4
S3-30	1.540	80	30	96.3
S3-300	1.550	350	300	97.7

3 TRIAXIAL EXPERIMENTS

A total of six ATC experiments were performed on the three sand types (Table 1). Each sand type was tested under drained conditions at two back pressures, maintaining a similar effective confining pressure (σ_3') of approximately 50 kPa. A high BP of 300 kPa was used to represent a typical laboratory testing conditions, while a ~30 kPa BP was used to mimic field

conditions. The ATC experiments on saturated sands were conducted using a miniature triaxial apparatus (Figure 1) that fits within the SMT scanning stage (Elnur and Alshibli, 2024). The cylindrical specimens had a diameter of 10.4 mm and a height of ~21 mm, encased inside a 0.33 mm-thick latex membrane. The smaller-than-typical size of the specimen was due to the limited size of the X-ray beam while scanning at a high resolution. The fluid used to saturate the specimen was a 4% (by mass) potassium iodide (KI) solution dissolved in deionized water, improving the x-ray attenuation contrast between air and water phases. The water and KI solution was first deaired using a vacuum pump and a hotplate, then pumped into the specimen using a GEOTAC DigiFlow pump. The pump allows the control and measurement of flow rates as low as 0.000025 ml/min to maintain the applied back pressure during shearing.

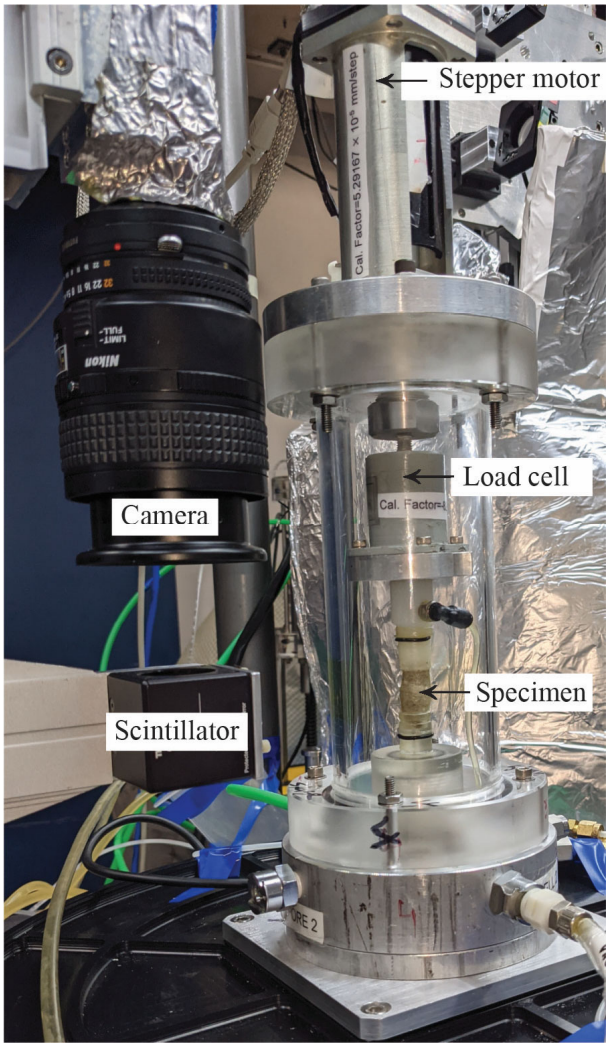

Figure 1. Mini-triaxial apparatus with a sheared specimen on the beamline 13D stage, Advanced Photon Source (APS).

The saturation stage consisted of pushing the KI solution at a flow rate of 0.2 - 0.4 ml/min, depending on pore pressure measurement, to prevent liquefaction and disturbance of the specimen. The KI solution was injected from the bottom to the top of the specimen to purge air from the specimen's pore space through the top-end cap. A sufficient de-aired solution volume (at least three times the specimen's pore volume) was applied through the specimen's pore space to purge air and increase the degree of saturation. After ensuring pressure stabilization, the specimen was compressed at a constant displacement rate of 0.025 mm/min.

4 SYNCHROTRON MICRO-COMPUTED TOMOGRAPHY (SMT) IMAGES

4.1 *Image Acquisition*

The 3D SMT images of the ATC experiments reported were acquired using GSECARS bending magnet beamline 13D (13 BM-D) at APS, Argonne National Laboratory (ANL), Illinois, USA. A white beam was filtered using a copper filter and reflected from a platinum-coated mirror, resulting in a pink beam with a reduced energy range (Elnur and Alshibli, 2023). Projected 2D images of specimens were collected at exposure times ranging from 6 to 12 milliseconds for 180° rotation, to obtain a 3D image. The spatial resolutions of the 3D SMT images ranged between 6.67 µm/voxel and 8.32 µm/voxel. Multiple SMT images were captured at various stages, including the initial dry state, flow stage, pressurizing stage, and different axial strains during the loading stage. The pink beam setup enabled quick image acquisition, removing the need to pause loading during scans and allowing specimen shearing without interruption. High-resolution scans, however, have a limited field of view, making it impossible to capture the entire height of the specimen in a single scan. The scanning stage uses a hexapod that moves the triaxial apparatus vertically while keeping the X-ray beam and camera at a fixed position. The complete height of the specimen was scanned into four overlapping stacks.

4.2 *Image processing*

The acquired 2D SMT radiographes were initially processed for dark field correction, flat field correction, zinger removal, and image reconstruction to acquire 3D greyscale image. The images of the four stacks were then merged to obtain a single 3D SMT grayscale image of the entire specimen. Images were then filtered using an anisotropic diffusion filter to enhance the image contrast and reduce noise. The grayscale value range for each phase (solids, KI solution, and air) was identified from the data histogram after filtering. The identified ranges were then used to obtain a 3D image of each phase by assigning a value of 1 to voxels within the targeted range and a value of 0 to voxels with values outside the range. and the filtered grayscale images were binarized by assigning a value of 1 for the targeted phase and 0 for the other two phases using an interactive thresholding module. The binary image of each phase was then used to calculate the volume of the phase by multiplying the number of non-zero voxels in the 3D binary image by the voxel's scale factor (resolution), hence obtaining the volume of solids (V_s), volume of water (V_w), and volume of air (V_a) (Imseeh et al., 2018). These measurements combined with the change in specimen height measurement form the scans allowed for assessment of volumetric strain (ε_v), axial strain (ε_1), and S at each scan.

5 ANALYSIS

The results of the 6 ATC experiments were first analyzed based on conventional measurement systems. Measurements of load and displacement from the data acquisition system, combined with pore water pressure and volume change measurements from the pump system, were used to calculate axial and volumetric strains, effective major principal stress (σ_1'), and the effective principal stress ratio ($EPSR$) using Equation (1).

$$EPSR = \frac{\sigma_1'}{\sigma_3'} \quad (1)$$

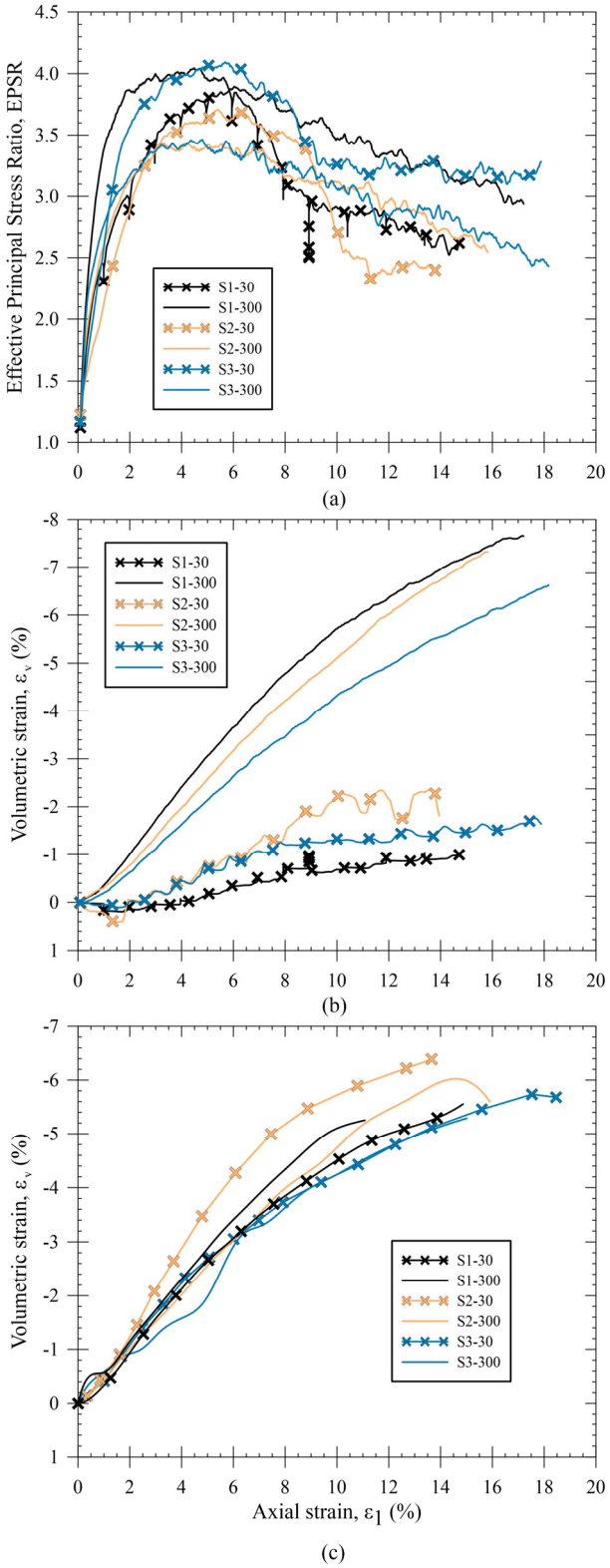

Figure 2. Evolution of (a) effective principal stress ratio; (b) volumetric strain based on pump measurements, and (c) volumetric strain based on 3D-SMT scans versus axial strain.

The evolution of EPSR versus axial strain results shown in Figure 2a reflected a higher peak strength for low BP experiments compared to high BP experiments, except for S1 sand, due to not achieving the target cell pressure and having a lower effective cell pressure of 44 kPa. Unlike the stress-strain curves that showed no distinct patterns, the volumetric strain evolution with loading from pump measurements (Figure 2b) showed a clear pattern where high BP pressure experiments exhibited a greater dilatancy and volumetric change compared to low BP experiments. Volumetric strains measured from 3D SMT images yielded the same results for high BP experiments as volumetric strains based on pump measurements; however, volumetric strains at low BP varied significantly between measurements from scans and the pump. Dilatancy behavior is associated with effective confining pressure (σ_3'), not total confining pressure (σ_3) (Chakraborty and Salgado, 2010). Hence, specimens with the same properties but tested under different back pressures are expected to exhibit the same volumetric behavior. Since all experiments were conducted at a similar effective confining pressure of approximately 50 kPa, the evolution of volumetric strain results from images were more consistent with tests conducted at similar effective confining pressure.

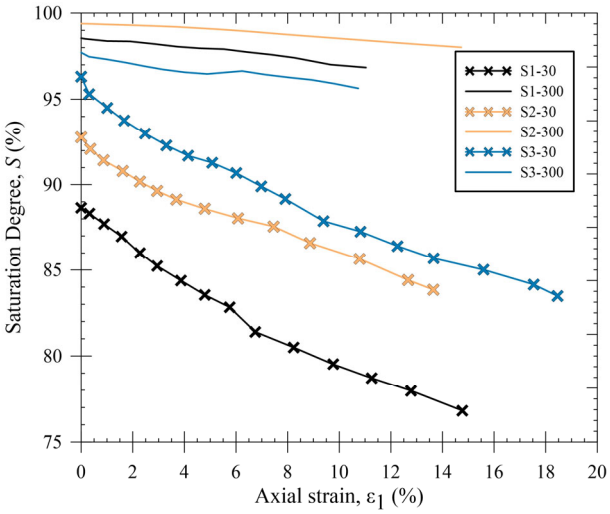

Figure 3. Evolution of the degree of saturation with axial strain

The evolution of the degree of saturation (S) with axial strain for all experiments is shown in Figure 3. High BP specimens had a higher initial S relative to low BP experiments (Table 1). This was in line with the typical use of high BP to saturate specimens, as the potential to eliminate air pockets by purging air out of the specimen and/or dissolving air into water increases with increasing BP. 3D SMT images revealed a higher frequency of trapped air pockets in low BP specimens. This suggests that the applied BP was not sufficient to dissolve entrapped air or overcome the air–water interfacial tension at the pore throats, allowing air to remain trapped within the specimen pore space (Brooks, 1965). Furthermore, 3D SMT scans of specimens tested under low BP revealed localized air pockets near the membrane at the specimen's bottom which is attributed to the mismatch between the specimen diameter (10.4 mm) and the diameter of the porous stone (6.3 mm). Even with the difficulty in achieving a high degree of saturation, *S2-30* and *S3-30* had an initial S high enough to be considered saturated. All specimens exhibited a reduction in S as shearing progressed. This reduction was minor in the case of high BP experiments. However, low BP specimens had a more significant reduction ($\Delta S > 10\%$) indicating an increase in air volume within the specimen. This accounts for the discrepancy in volumetric strains observed between the pump-based and scan-based measurements. The specimen's volume change is estimated indirectly via pump outflow, based on the assumption that any increase in specimen volume directly matches the expelled fluid. However, this approach overlooks the internal expansion of air within the specimen, resulting in measurement divergence.

6 CONCLUSIONS

The results of drained ATC experiments on sands with different morphology and gradation at two different back pressures, representing a typical laboratory setup and field conditions, showed a behavior independent of morphology and gradation. The evolution of volumetric strain with axial strain based on SMT imaging aligned with the expectation for specimens tested at similar effective confining pressure, exhibiting similar volumetric and dilatancy behavior. In contrast, the conventional volume measurement system revealed a drastically different behavior due to its failure to capture the volume change of air within the specimen. The increase in air volume for low back pressure specimens was significant enough to lower the degree of saturation below 85% indicating a potential transition from saturated to unsaturated framework. The assumption that laboratory tests, which are typically conducted under high back pressure, justify the use of saturated soil mechanics raises concerns about the reliability of derived parameters—especially for specimens exhibiting dilative behavior—when applied to field conditions where pore water pressure is low. This discrepancy calls into question the extent to which laboratory-based interpretations reflect in situ soil responses, particularly for zones just below the groundwater table.

7 ACKNOWLEDGEMENTS

This material was partially funded by the U.S. National Science Foundation (NSF) under Grant No. CMMI-2016392. Any opinions, findings, conclusions, and recommendations expressed in this paper are those of the authors and do not necessarily reflect the views of the NSF. The SMT scans presented in this paper were collected using the X-Ray Operations and Research Beamline Station 13-BMD of the Advanced Photon Source (APS), a U.S. Department of Energy (DOE) Office of Science User Facility operated by the Argonne National Laboratory (ANL) under Contract No. DE-AC02-06CH11357. We acknowledge the support of GeoSoilEnviroCARS (Sector 13), which is funded by the NSF Earth Sciences (EAR-1128799) and the DOE Geosciences (DE-FG02-94ER14466). We thank Dr. Mark Rivers for his guidance at APS.

8 REFERENCES

Alshibli, K.A. et al. 2015. Quantifying morphology of sands using 3D imaging. *Journal of Materials in Civil Engineering* 27(10) 04014275.

ASTM D7181-20: Standard Test Method for Consolidated Drained Triaxial Compression Test for Soils. West Conshohocken, PA, ASTM International, 2020.

Bishop, A.W., Alpan, I., Blight, G. and Donald, I. 1960. Factors controlling the strength of partly saturated cohesive soils.

Brooks, R.H. 1965. *Hydraulic properties of porous media*: Colorado State University.

Chakraborty, T. and Salgado, R. 2010. Dilatancy and shear strength of sand at low confining pressures. *Journal of geotechnical and geoenvironmental engineering* 136(3) 527-532.

Elnur, M. and Alshibli, K.A. 2023. Influence of X-Ray Beam Exposure on the Development of Gas Bubbles During Triaxial Testing of Sand Using 3D Synchrotron Micro-Computed Tomography. *Tomography of Materials and Structures* 100016.

Elnur, M. and Alshibli, K.A. 2024. Experimental investigation of the influence of drainage condition on change in saturation of sheared sand. *Géotechnique* 1-19.

Fredlund, D.G. 2019. State of practice for use of the soil-water characteristic curve (SWCC) in geotechnical engineering. *Canadian Geotechnical Journal* 56(8) 1059-1069.

Imseeh, W.H., Druckrey, A.M. and Alshibli, K.A. 2018. 3D experimental quantification of fabric and fabric evolution of sheared granular materials using synchrotron micro-computed tomography. *Granular Matter* 20(2) 1-28.

Kido, R. and Higo, Y. 2017. Evaluation of distribution of void ratio and degree of saturation in partially saturated triaxial sand specimen using micro x-ray tomography. *Japanese Geotechnical Society Special Publication* 5(2) 22-27.

Lloret-Cabot, M. et al. 2018. From saturated to unsaturated conditions and vice versa. *Acta Geotechnica* 13 15-37.

Skempton, A. 1954. The pore-pressure coefficients A and B. *Géotechnique* 4(4) 143-147.

Takano, D., Lenoir, N., Otani, J. and Hall, S.A. 2015. Localised deformation in a wide-grained sand under triaxial compression revealed by X-ray tomography and digital image correlation. *Soils and foundations* 55(4) 906-915.

Vanapalli, S., Fredlund, D., Pufahl, D. and Clifton, A. 1996. Model for the prediction of shear strength with respect to soil suction. *Canadian Geotechnical Journal* 33(3) 379-392.